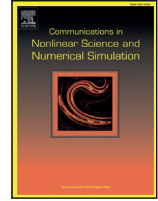




Contents lists available at ScienceDirect

Commun Nonlinear Sci Numer Simulat

journal homepage: www.elsevier.com/locate/cnsns

Research paper

Analysis and simulation of periodic and solitary waves in nonlinear dispersive-dissipative solids



Xianbo Sun, Yanni Zeng, Pei Yu*

Department of Applied Mathematics, Western University, London, Ontario, N6A 5B7, Canada

ARTICLE INFO

Article history:

Received 23 January 2021

Revised 10 June 2021

Accepted 11 June 2021

Available online 15 June 2021

Keywords:

Nonlinear dispersive-dissipative solids

Periodic traveling wave

Melnikov function

Homoclinic cycle

Geometric singular perturbation theory

Chebyshev criterion

ABSTRACT

In this paper, we consider a general realistic nonlinear elastic rod model which is embedded in an external medium with weak disturbance. We apply the geometric singular perturbation theory to prove the existence of a unique periodic traveling wave in this model. With a dynamical system approach, it is shown that the periodic wave appears near a stationary state and then amplifies and degenerates into a solitary wave. Simulations are presented to demonstrate an excellent agreement with the theoretical predictions.

© 2021 Elsevier B.V. All rights reserved.

1. Introduction

In material science, it is very important to assess the durability of materials and structures. One efficient way to assess the durability of elastic materials is to study the long quasi-stationary and localized strain waves that propagate over long distance along elastic waveguides, because the waves transfer energy during their propagation. The strain waves may be deformed, amplified or broken due to the inhomogeneity in the waveguide or due to the influence of externally dissipative medium on the waveguide lateral surface. Dissipative effects may arise from the internal features of the elastic material. Since in reality dissipation always exists, which may be caused by internal features of the elastic material, an irreversible part should be included into the stress tensor in addition to the reversible one depending only upon the density of the Helmholtz energy [1]. Consequently, the governing equations should contain viscoelastic terms in the strains. Another type of dissipation may also occur on the lateral surface of an elastic waveguide, for example, Kerr [2] proposed a viscoelastic model describing an elastic body which involves external snow (or permafrost) medium.

In this paper, our study is focused on a particular physical problem, formulated by Porubov and Velarde [3], to investigate the propagation of a longitudinal strain wave in an isotropic cylindrical elastic rod, which is embedded in an external medium. For the convenience of readers, we take the modeling formulas from [3] to outline the description of the problem as follows. In [3], the cylindrical coordinates (x, r, ϕ) and the displacement vector $V = (u, w, 0)$ are used to derive the equation, for which the torsion is neglected, where $x \in (-\infty, +\infty)$ is along the axis of the rod, r is the radial coordinate, and

* Corresponding author.

E-mail address: pyu@uwo.ca (P. Yu).

$\phi \in [0, 2\pi]$ is a polar angle. Then the Green-Lagrange strain tensor is defined by

$$C = \frac{[\nabla V + (\nabla V)^T + \nabla V(\nabla V)^T]}{2}, \tag{1}$$

where T denotes transpose. The externally dissipative medium yields a normal stress P_{rr}^* on the lateral surface of the rod at $r = R$,

$$P_{rr}^* = -\frac{k}{r}w - \eta w_t + \chi r^2 w_{xxt}, \tag{2}$$

where t, k, η and χ represent time, the stiffness measure or the compressibility coefficient, the visco-compressibility coefficient and the viscosity coefficient of the external medium, respectively.

Suppose the deformation is adiabatic, then the Lagrangian density L is measured by the difference between the bulk density of the internal energy Π and the kinetic energy density K , described by

$$L = K - \Pi = \frac{\rho_0}{2} \left[\left(\frac{\partial w}{\partial t} \right)^2 + \left(\frac{\partial u}{\partial t} \right)^2 \right] - \Pi(I_k), \tag{3}$$

where ρ_0 denotes the material density of the rod at t_0 , I_k ($k = 1, 2, 3$) is the invariant of the tensor C , given by

$$I_1(C) = \text{Tr} C, \quad I_2(C) = \frac{(\text{Tr} C)^2 - \text{Tr} C^2}{2}, \quad I_3(C) = \det(C).$$

The strain-induced thermodynamic changes are neglected because of weak strains. Then, Π is evaluated by the following potential strain energy density according to Murnaghan's approximation, which has accurate applicability to a wide class of nonlinear elastic materials [4,5],

$$\Pi = \frac{\lambda + 2\mu}{2} I_1^2 - 2\mu I_2 + \frac{l + 2m}{3} I_1^3 - 2m I_1 I_2 + n I_3, \tag{4}$$

where λ and μ are Lamé coefficients, characterizing the linear elastic properties of the isotropic material, while l, m and n represent the Murnaghan moduli which account for nonlinear elastic properties of the isotropic material. Note that λ and μ only take positive values. Then, by imposing the boundary conditions to the action functional, we have

$$\delta S = \delta \int_{t_0}^{t_1} dt \left[2\pi \int_{-\infty}^{+\infty} dx \int_0^R r L dr + 2\pi \int_{-\infty}^{+\infty} P_{rr}^* w dx \right]. \tag{5}$$

Porubov and Velarde [3] applied Hamilton's principle and variational analysis to derive the following equation via a series of substitutions (see [3] for more details):

$$v_{tt} - \alpha_1 v_{xx} - \alpha_2 v_{xxt} - \alpha_3 (v^2)_{xx} - \alpha_4 v_{xxxx} + \alpha_5 v_{xxtt} - \alpha_6 (v^2)_{xxt} - \alpha_7 v_{xxxxt} + \alpha_8 v_{xxttt} = 0, \tag{6}$$

where the coefficients $\alpha_i, i = 1, 2, \dots, 8$, are given in Appendix B of [3]. An exact analytic solitary wave solution was obtained in (6) under the following constraint [3]:

$$\alpha_6(\alpha_4\alpha_6 - \alpha_3\alpha_7) = (\alpha_1\alpha_6 - \alpha_2\alpha_3)(\alpha_5\alpha_6 - \alpha_3\alpha_8).$$

Now we consider possible wave solutions in the general system (6). Without any additional assumptions, finding traveling wave solutions in system (6) becomes extremely difficult. However, if the external dissipative medium is assumed to be weak, which is often observed in reality [3], then all the coefficients of the dissipative terms in (6) are small relative to the other ones and can be expressed in the form of $\alpha_2 = \epsilon\beta_2, \alpha_6 = \epsilon\beta_6, \alpha_7 = \epsilon\beta_7, \alpha_8 = \epsilon\beta_8, (0 < \epsilon \ll 1)$ under which (6) becomes

$$v_{tt} - \alpha_1 v_{xx} - \alpha_3 (v^2)_{xx} - \alpha_4 v_{xxxx} + \alpha_5 v_{xxtt} = \epsilon (\beta_2 v_{xxt} + \beta_6 (v^2)_{xxt} + \beta_7 v_{xxxxt} - \beta_8 v_{xxttt}). \tag{7}$$

Even under the above assumption, it is still very difficult to find a wave solution or even just prove the existence of a wave solution in system (7). With a numerical verification, Porubov and Velarde [3] have demonstrated that equation (7) possesses a solitary which tends to the solitary of system (7) as $\epsilon \rightarrow 0$. Nevertheless, the following questions are still open:

1. Can the equation (7) have periodic wave solutions?
2. If equation (7) has periodic wave solutions, then what kind of balance exists between the externally dissipative medium and the nonlinearity, which controls the periodic and solitary waves.

In this paper, we will apply the Geometric Singular Perturbation Theory (GSPT) [6] to provide a rigorous proof for the existence of a unique periodic wave in equation (7). We will also show that as the parameters are varied in a range of the ratio of two elliptic integrals, the periodic wave appears near a constant stationary state and then amplifies and degenerates into a solitary wave. Our these results answer the above two open questions. The novelty of our method is that the method is not only applicable for proving the existence of a unique wave solution, but can also be easily generalized to deal with the case with multiple wave solutions.

Periodic travelling wave is related to a spatio-temporal oscillation phenomenon in many real word problems described by partial differential equations (PDE), which is a particular type of non-uniform distribution, in which the related quantity or

density varies periodically in one spatial direction, as well as in time, exhibiting a wave in a combined spatial and temporal oscillation. When a PDE model is transformed to an ordinary differential equation (ODE) model, a periodic orbit in the ODE model corresponds to a wave solution in the PDE model. In particular, a periodic travelling wave in one dimensional PDE corresponds to a limit cycle in its associated ODE system. However, the Lyapunov stability of the limit cycle does not necessarily imply the stability of the corresponding periodic travelling wave. In fact, it has been shown that [7,8] the stability of periodic travelling wave depends partially on its amplitude, i.e., a periodic travelling wave with sufficiently low amplitude is unstable even if the travelling wave equation has supercritical Hopf bifurcation.

The GPST is widely applied to study differential dynamical systems involving multiple time scales, which exhibit slow-fast motions, and such a system is usually called singular perturbation system [6]. For an illustration, consider the following 2-dimensional dynamical system:

$$\frac{dx_1}{dt} = f(x_1, x_2, \varepsilon), \quad \frac{dx_2}{dt} = \varepsilon g(x_1, x_2, \varepsilon), \quad (8)$$

where $(x_1, x_2) \in \mathbb{R}^2$, $0 < \varepsilon \ll 1$, and $f, g \in C^k$, $k \geq 3$, x_1 and x_2 are called fast and slow variables. Introducing $\tau = \varepsilon t$ into (8) yields

$$\varepsilon \frac{dx_1}{d\tau} = f(x_1, x_2, \varepsilon), \quad \frac{dx_2}{d\tau} = g(x_1, x_2, \varepsilon). \quad (9)$$

Here, the systems (8) and (9) are called fast and slow systems, respectively with the fast time t and the slow time τ . To study slow-fast motions in systems (8) and (9), the basic idea is to first consider their limiting systems as $\varepsilon \rightarrow 0$, yielding the fast subsystem,

$$\frac{dx_1}{dt} = f(x_1, x_2, 0), \quad \frac{dx_2}{dt} = 0, \quad (10)$$

and the slow subsystem,

$$0 = f(x_1, x_1, 0), \quad \frac{dx_2}{d\tau} = g(x_1, x_2, 0), \quad (11)$$

respectively. Note that the singular points of the fast subsystem (10), determined by the equation $f(x_1, x_2, 0) = 0$, defines a critical manifold, also called slow manifold. It is easy to see that the fast subsystem defines a fast manifold in the horizontal direction. Therefore, if the fast and slow manifolds can form a closed loop, then the system (8) may exhibit slow-fast periodic motions (e.g., canard cycle) under a small perturbation.

The Bogdanov-Takens (B-T) bifurcation is associated with a double-zero eigenvalue in dynamical systems (for example see [9–11]). Besides the popular Hopf bifurcation, the B-T bifurcation also plays an very important role in the study of dynamical behaviours of nonlinear systems. It is well known that even for codimension-two B-T bifurcation, saddle-node bifurcation, Hopf bifurcation and Homoclinic loop bifurcation can occur near a critical point. In particular, the Homoclinic loop bifurcation is analyzed by using the Melnikov function method with proper scaling. This establishes the relation between the B-T bifurcation and the general bifurcation in near-Hamiltonian systems. Certainly, using B-T bifurcation to study a near-Hamiltonian system is only applicable if there exists a B-T equation which matches the near-Hamiltonian system.

In a recently published article [12], the GSPT has been applied to study the coexistence of solitary and periodic waves in convecting shallow water fluid. But it should be noted that the two Alebian integrals considered in [12] have monotone property which makes the proof easy, while that in this paper do not have this property. Moreover, in this paper when proving the existence of a unique zero of the ratio of two Alebian integrals, we first apply the classical codimension-two B-T bifurcation theory [13] and then use the geometric approach with the Chebyshev criterion [14], giving a comparison to show that the geometric method is better and simpler than the method based on the classical B-T bifurcation theory. Our this contribution proves a better method for studying traveling wave solutions in PDEs and promotes further development in this research area.

In the next section, we perform a reduction analysis which transforms system (7) to a singularly perturbed ODE system, yielding two perturbed Hamiltonian systems. In Section 3, we prove the existence of a unique limit cycle in the reduced ODE system, which corresponds to a unique wave solution of system (7). Two proofs are provided: One is based on the classical B-T bifurcation theory with the equation given in [13], and the other is based on a dynamical system approach with the Chebyshev criterion. Their comparison shows the advantage of the latter, which is better and simpler than the former. Then, in Section 4, the theoretical results are applied to numerical examples of system (7) with the real data taken from [3]. In fact, it was assumed in [3] that an analytic wave solution exists and then the authors applied expansion to find approximate solutions. Numerical simulations were also given in [3] to illustrate the analytic predictions. We will use the theoretical results to prove the existence of a unique wave solution and present simulation to verify the prediction. Finally, conclusion is drawn in Section 5.

2. Reduction of equation (7)

In this section, the traveling wave problem for the isotropic cylindrical elastic rod embedded in an externally dissipative medium is reduced into a singular perturbation problem. We first show that the related critical manifold is normally

hyperbolic, and then restrict the analysis on the hyperbolic critical manifold to form a regular perturbation problem. For the regularly perturbed model, we construct the Melnikov function on the whole Hamiltonian-periodic structure, and consider its zeros globally. The existence and uniqueness of the zero implies that a unique periodic wave can emerge from the original integrable structure.

First, introducing the wave profile $z = x - ct$ into equation (7) and integrating it twice we obtain a 3rd-order ODE:

$$(c^2 - \alpha_1)v - \alpha_3v^2 + (c^2\alpha_5 - \alpha_4)v_{zz} = -c\epsilon\beta_2v_z - 2c\epsilon\beta_6vv_z + \epsilon(c^3\beta_8 - c\beta_7)v_{zzz}. \tag{12}$$

We assume that $c > 0$, and that the boundary conditions satisfy

$$\lim_{z \rightarrow \infty} \frac{dv}{dz} = \lim_{z \rightarrow \infty} \frac{d^2v}{dz^2} = \lim_{z \rightarrow \infty} \frac{d^3v}{dz^3} = 0.$$

Equation (12) can be rewritten as an equivalent dynamical system,

$$\begin{aligned} \frac{dv}{dz} &= y, \\ \frac{dy}{dz} &= w, \\ \epsilon(c^3\beta_8 - c\beta_7) \frac{dw}{dz} &= (c^2 - \alpha_1)v - \alpha_3v^2 + (c^2\alpha_5 - \alpha_4)w + \epsilon c\beta_2y + 2\epsilon c\beta_6vy, \end{aligned} \tag{13}$$

which is singular at $\epsilon = 0$, since the solution does not converge uniformly as $\epsilon \rightarrow 0$ to a singular solution for $\epsilon = 0$. Further, introducing a relatively fast time scale $\zeta = z/\epsilon$ into the above system, we have

$$\begin{aligned} \frac{dv}{d\zeta} &= \epsilon y, \\ \frac{dy}{d\zeta} &= \epsilon w, \\ (c^3\beta_8 - c\beta_7) \frac{dw}{d\zeta} &= (c^2 - \alpha_1)v - \alpha_3v^2 + (c^2\alpha_5 - \alpha_4)w + \epsilon c\beta_2y + 2\epsilon c\beta_6vy, \end{aligned} \tag{14}$$

which is equivalent to systems (13) for $\epsilon > 0$, and both systems (13) and (14) are singular perturbation systems. System (13) is usually called slow-subsystem since the scaled time z is slow, and system (14) is referred as fast-subsystem because time ζ is fast. Equations (13) and (14) have the following limiting forms as $\epsilon \rightarrow 0$:

$$\begin{aligned} \frac{dv}{dz} &= y, \\ \frac{dy}{dz} &= w, \\ 0 &= (c^2 - \alpha_1)v - \alpha_3v^2 + (c^2\alpha_5 - \alpha_4)w, \end{aligned} \tag{15}$$

and

$$\begin{aligned} \frac{dv}{d\zeta} &= 0, \\ \frac{dy}{d\zeta} &= 0, \\ (c^3\beta_8 - c\beta_7) \frac{dw}{d\zeta} &= (c^2 - \alpha_1)v - \alpha_3v^2 + (c^2\alpha_5 - \alpha_4)w, \end{aligned} \tag{16}$$

respectively. The slow system (15) is a differential-algebraic system and its flow can be confined to the set,

$$\mathcal{M}_0 = \{(v, y, w) \in \mathbb{R}^3 \mid (c^2 - \alpha_1)v - \alpha_3v^2 + (c^2\alpha_5 - \alpha_4)w = 0\}, \tag{17}$$

which is the equilibrium set of system (16). \mathcal{M}_0 is a two-dimensional critical (slow) manifold.

In classical GSPT [6], the connected components of the critical manifold \mathcal{M}_0 are said normally hyperbolic if each equilibrium point in the component of system (16) is hyperbolic. When the critical manifold is normally hyperbolic, there exists a normally hyperbolic, slow manifold \mathcal{M}_ϵ , which approaches \mathcal{M}_0 in Hausdorff distance as $\epsilon \rightarrow 0$. The flow of (13) can be projected onto the slow manifold \mathcal{M}_ϵ , and then the singular perturbation model is usually reduced to a regular perturbation problem, see more details in [6].

The linearized matrix of the fast system (14) restricted to \mathcal{M}_0 is given by

$$\begin{bmatrix} 0 & 0 & 0 \\ 0 & 0 & 0 \\ 0 & 0 & (c^2 - \alpha_1) - 2\alpha_3v & 0 & c^2\alpha_5 - \alpha_4 \end{bmatrix}$$

which has no purely imaginary eigenvalues. Therefore, \mathcal{M}_0 is normally hyperbolic by Fenichel's criterion (pages 74-75 in [6]). Hence, the critical manifold \mathcal{M}_0 persists as a two-dimensional slow manifold \mathcal{M}_ϵ for sufficiently small ϵ .

Suppose w , restricted to \mathcal{M}_ϵ , can be expressed as

$$w = -\frac{(c^2 - \alpha_1)v - \alpha_3v^2}{(c^2\alpha_5 - \alpha_4)} + \epsilon \Theta_0(v, y) + \epsilon \sum_{i=1}^{\infty} \Theta_i(v, y)\epsilon^i. \tag{18}$$

Then we have

$$\mathcal{M}_\epsilon = \left\{ (v, y, w) \in \mathbb{R}^3 \mid w = -\frac{(c^2 - \alpha_1)v - \alpha_3v^2}{(c^2\alpha_5 - \alpha_4)} + \epsilon \Theta_0(v, y) + \epsilon \sum_{i=1}^{\infty} \Theta_i(v, y)\epsilon^i \right\}. \tag{19}$$

Substituting (18) into the slow system (13) yields

$$\begin{aligned} & \epsilon(c^3\beta_8 - c\beta_7) \frac{(\alpha_1 - c^2 + 2\alpha_3v)y}{(c^2\alpha_5 - \alpha_4)} + O(\epsilon^2) \\ = & (c^2 - \alpha_1)v - \alpha_3v^2 + \epsilon c\beta_2y + 2\epsilon c\beta_6vy \\ & + (c^2\alpha_5 - \alpha_4) \left[-\frac{(c^2 - \alpha_1)v - \alpha_3v^2}{(c^2\alpha_5 - \alpha_4)} + \epsilon \Theta_0(v, y) + \epsilon \sum_{i=1}^{\infty} \Theta_i(v, y)\epsilon^i \right] + O(\epsilon^2). \end{aligned} \tag{20}$$

Comparing the coefficient of ϵ on both sides of (20), we obtain

$$\Theta_0(u, v) = (l_0 + l_1v)y, \tag{21}$$

where

$$\begin{aligned} l_0 &= \frac{(c^3\beta_8 - c\beta_7)(\alpha_1 - c^2) - c\beta_2(c^2\alpha_5 - \alpha_4)}{(c^2\alpha_5 - \alpha_4)^2}, \\ l_1 &= \frac{2(c^3\beta_8 - c\beta_7)\alpha_3 - 2c\beta_6(c^2\alpha_5 - \alpha_4)}{(c^2\alpha_5 - \alpha_4)^2}. \end{aligned} \tag{22}$$

Then, system (13) projected on \mathcal{M}_ϵ has the form,

$$\begin{aligned} \frac{dv}{dz} &= y, \\ \frac{dy}{dz} &= \frac{(\alpha_1 - c^2)v + \alpha_3v^2}{(c^2\alpha_5 - \alpha_4)} + \epsilon(l_0 + l_1v)y + O(\epsilon^2). \end{aligned} \tag{23}$$

When $\frac{\alpha_1 - c^2}{c^2\alpha_5 - \alpha_4} < 0$, introducing the transformations: $v = s\tilde{v}$, $y = a_1\tilde{y}$, $z = b_1\tilde{\xi}$ and $\tilde{\epsilon} = b_1\epsilon$, where

$$s = -\frac{\alpha_1 - c^2}{\alpha_3}, \quad b_1 = \left(\frac{c^2 - \alpha_1}{c^2\alpha_5 - \alpha_4} \right)^{-\frac{1}{2}}, \quad a_1 = \frac{s}{b_1}, \tag{24}$$

into (23) we obtain the following dimensionless system (in which the tilde notation has been dropped for simplicity),

$$\begin{aligned} \frac{dv}{d\tilde{\xi}} &= y, \\ \frac{dy}{d\tilde{\xi}} &= -v(1 - v) + \epsilon(\gamma_0 + \gamma_1v)y, \end{aligned} \tag{25}$$

where

$$\gamma_0 = l_0, \quad \gamma_1 = sl_1 \tag{26}$$

in which l_0 and l_1 are given in (22). System (25) $_{\epsilon=0}$ is a Hamiltonian system with the Hamiltonian,

$$H(v, y) = \frac{y^2}{2} + \frac{v^2}{2} - \frac{v^3}{3}.$$

When $\frac{\alpha_1 - c^2}{c^2\alpha_5 - \alpha_4} > 0$, we introduce $v = s\tilde{v}$, $y = a_2\tilde{y}$, $z = b_2\tilde{\xi}$ and $\tilde{\epsilon} = b_2\epsilon$ with

$$s = -\frac{\alpha_1 - c^2}{\alpha_3}, \quad b_2 = \left(\frac{\alpha_1 - c^2}{c^2\alpha_5 - \alpha_4} \right)^{-\frac{1}{2}}, \quad a_2 = \frac{s}{b_2},$$

into (23) to obtain the dimensionless system (with tilde dropped),

$$\begin{aligned} \frac{dv}{d\tilde{\xi}} &= y, \\ \frac{dy}{d\tilde{\xi}} &= v(1 - v) + \epsilon(\gamma_0 + \gamma_1v)y, \end{aligned} \tag{27}$$

where γ_0 and γ_1 are given in (26). System (27) $_{\epsilon=0}$ is also a Hamiltonian system with the Hamiltonian

$$H^*(v, y) = \frac{y^2}{2} - \frac{v^2}{2} + \frac{v^3}{3}.$$

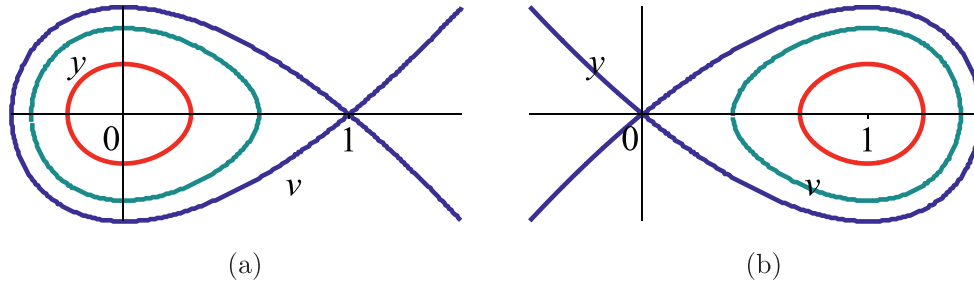


Fig. 1. (a) phase portrait of systems (25)_{ε=0}; and (b) phase portrait of systems (27)_{ε=0}, where the homoclinic loops (in blue color) correspond to two types of solitary waves of the model (7)_{ε=0}.

Systems (25) and (27) are near-Hamiltonian systems, and the two homoclinic loops associated with the systems (25)_{ε=0} and (27)_{ε=0} are defined by $H(v, y) = \frac{1}{6}$ and $H^*(v, y) = 0$, respectively, as shown in Figure 1. The two homoclinic loops correspond to the solitary waves of the original model (7)_{ε=0} (without dissipative medium).

It should be noted that the two near-Hamiltonian systems (25) and (27) are equivalent under the following transformation (from system (27) to (25)):

$$v \rightarrow 1 - v, \quad y \rightarrow y, \quad \xi \rightarrow -\xi, \quad -(\gamma_0 + \gamma_1) \rightarrow \gamma_0, \quad \gamma_1 \rightarrow \gamma_1. \tag{28}$$

Thus, we will only prove the existence of periodic waves associated with system (25), and all the simulations are presented for this system.

For system (25)_{ε=0}, there is a family of periodic orbits Γ_h defined by $\{(v, y) | H(v, y) = h, h \in (0, \frac{1}{6})\}$. Let $(v, y) = (\rho(h), 0)$ denote the intersection point of the periodic orbit Γ_h with the positive v -axis, T be the period of the periodic orbit Γ_h . Further, suppose that $\Gamma_{h,\epsilon}$ is an orbit of (25) starting from $(\rho(h), 0)$ at time $\xi = 0$, and first intersecting the positive v -axis at $(\pi(h, \epsilon), 0)$ at time $\xi = \xi(\epsilon)$. Then, the difference between the two intersection points can be expressed as

$$\begin{aligned} \int_{\Gamma_{h,\epsilon}} dH &= H(\pi(h, \epsilon), 0) - H(\rho(h), 0) = \int_{\Gamma_{h,\epsilon}} v(1-v)dv + ydy \\ &= \int_0^{\xi(\epsilon)} \{v(1-v)y + y[-v(1-v) + \epsilon(\gamma_0 + \gamma_1 v)y]\} d\xi \\ &= \epsilon \int_0^{\xi(\epsilon)} (\gamma_0 + \gamma_1 v)y^2 d\xi \triangleq \epsilon \mathcal{F}(h, \epsilon). \end{aligned}$$

By theorem of continuousness function, we have

$$\lim_{\epsilon \rightarrow 0} \Gamma_{h,\epsilon} = \Gamma_h, \quad \lim_{\epsilon \rightarrow 0} \pi(h, \epsilon) = \rho(h), \quad \lim_{\epsilon \rightarrow 0} \xi(\epsilon) = T,$$

and thus,

$$\mathcal{F}(h, \epsilon) = \int_0^T (\gamma_0 + \gamma_1 v)y^2 d\xi + O(\epsilon) = \oint_{\Gamma_h} (\gamma_0 + \gamma_1 v)ydv + O(\epsilon). \tag{29}$$

Define

$$\mathcal{M}(h, \gamma_0, \gamma_1) = \oint_{\Gamma_h} (\gamma_0 + \gamma_1 v)ydv, \tag{30}$$

which is called (the first-order) Melnikov function constructed on the whole periodic structure of system (25)_{ε=0}.

Similarly, we can construct a Melnikov function for system (27) on the periodic annulus $\{\Gamma_h^*\} = \{(v, y) | H^*(v, y) = h, h \in (-\frac{1}{6}, 0)\}$, given by

$$\mathcal{M}^*(h, \gamma_0, \gamma_1) = \oint_{\Gamma_h^*} (\gamma_0 + \gamma_1 v)ydv. \tag{31}$$

In the next section, we will establish the existence of a unique zero of the Melnikov functions $\mathcal{M}(h, \gamma_0, \gamma_1)$ in $h \in (0, \frac{1}{6})$.

3. Existence of periodic waves in model (7)

In this section, we show that the Melnikov function $\mathcal{M}(h, \gamma_0, \gamma_1)$ has a unique zero in $h \in (0, \frac{1}{6})$. $\mathcal{M}(h, \gamma_0, \gamma_1)$ can be rewritten as

$$\mathcal{M}(h, \gamma_0, \gamma_1) = \gamma_0 m_0(h) \left(1 + \frac{\gamma_1 m_1(h)}{\gamma_0 m_0(h)} \right), \tag{32}$$

where

$$m_0(h) = \oint_{\Gamma_h} ydv, \quad m_1(h) = \oint_{\Gamma_h} ydv,$$

Note that

$$m_0(h) = \oint_{\Gamma_h} ydv = \iint_{\Omega} dvdy > 0,$$

by Green formula, where Ω is the region bounded by Γ_h . Therefore, $\frac{m_1(h)}{m_0(h)}$ is well defined in $(0, \frac{1}{6})$.

First, we use the classical B-T bifurcation theory to prove that $\mathcal{M}(h, \gamma_0, \gamma_1)$ has a unique zero in $h \in (0, \frac{1}{6})$, which needs a system having a double-zero eigenvalue at an equilibrium point to match our system (25) under an appropriate scaling. This system happens to exist in [13] and the results given in that article can be directly applied to prove that the Melnikov function for our system (25) has a unique zero, that is, there exists a unique limit cycle between the center (0,0) and the homoclinic loop passing through the saddle point (1,0). Then, we briefly describe a dynamical system approach based on the Chebyshev criterion [14], since this approach can be easily generalized to consider other more complex PDEs, while the traditional B-T bifurcation theory may not be applicable. The main idea of analyzing homoclinic cycles in B-T bifurcation is to take proper scaling and transform the system to a perturbed Hamiltonian system, and then apply the Abelian integral to prove the existence of the unique zero of the Melnikov function, which is certainly the same as the dynamical approach to directly analyze the Melnikov function for system (25). It should be pointed out that the B-T bifurcation theory is only applicable for the case in proving a unique zero of Melnikov function, it fails for the case when the Melnikov function has multiple zeros.

We take equation (1.1) from [13] and ignore the higher-order terms to obtain the following system,

$$\begin{aligned} \frac{dX}{dt} &= Y, \\ \frac{dY}{dt} &= \mu X + \nu Y + MX^2 + \Gamma XY, \end{aligned} \tag{33}$$

where $M \neq 0$, $\Gamma \neq 0$, and μ and ν are parameters. When $\mu = \nu = 0$, the linearized system of (33) has a double-zero eigenvalue at the origin. It is noted that the origin $(X, Y) = (0, 0)$ will not remain a singular point under general perturbation, and it does not hold symmetry. System (33) has a transcritical bifurcation, while the generic unfolding $\mu + \nu X$, instead of $\mu X + \nu Y$, yields a saddle-node bifurcation.

It is easy to show that system (33) has two equilibrium solutions $E_0 = (0, 0)$ and $E_1 = (-\mu, 0)$. Using a linear analysis we know that there exists a transcritical bifurcation at $\nu = 0$ between E_0 and E_1 . Hopf bifurcation occurs either from E_0 for $\mu < 0$ and from E_1 for $\mu > 0$. To prove the existence of limit cycles around E_0 , we take $\epsilon = \sqrt{-\mu}$, $\mu < 0$, $|\mu| \ll 1$. Further, introducing the following scales:

$$X = \epsilon^2 v, \quad Y = \epsilon^3 y, \quad \nu = \epsilon^2 \gamma_0, \quad \xi = \epsilon t, \tag{34}$$

into system (33) we obtain

$$\begin{aligned} \frac{dv}{d\xi} &= y, \\ \frac{dy}{d\xi} &= -\nu(1 - Mv) + \epsilon(\gamma_0 + \Gamma v)y. \end{aligned} \tag{35}$$

Now letting $M=1$ and $\Gamma = \gamma_1$ in system (35) leads to our system (25). The main task of the paper [13] is to prove that the Melnikov function M given in (25) has a unique zero by showing that the ratio function $\frac{m_1(h)}{m_0(h)}$ is monotonic. In [13] the authors applied the averaging theory and the elliptic integrals of the first and second kind to prove the monotonicity. Hence, we can directly apply the conclusion obtained in [13] and conclude that $\frac{m_1(h)}{m_0(h)}$ is monotonic.

In the following, we briefly present the dynamical system approach based on the Chebyshev criterion [14] to prove that $\frac{m_1(h)}{m_0(h)}$ is monotonic for $h \in (0, \frac{1}{6})$. To achieve this, let

$$\begin{aligned} U(v) &= H(v, y) - \frac{y^2}{2} = \frac{v^2}{2} - \frac{v^3}{3}, \\ L_i(v, Z) &= \frac{v^i}{U'(v)} - \frac{Z^i}{U'(Z)}, \quad \text{for } i = 0, 1, \end{aligned} \tag{36}$$

where Z is defined by $q(v, Z) = 0$, where

$$q(v, Z) = 2v^2 + 2vZ + 2Z^2 - 3v - 3Z, \tag{37}$$

satisfying

$$U(v) - U(Z) = -\frac{v-Z}{6} q(v, Z). \tag{38}$$

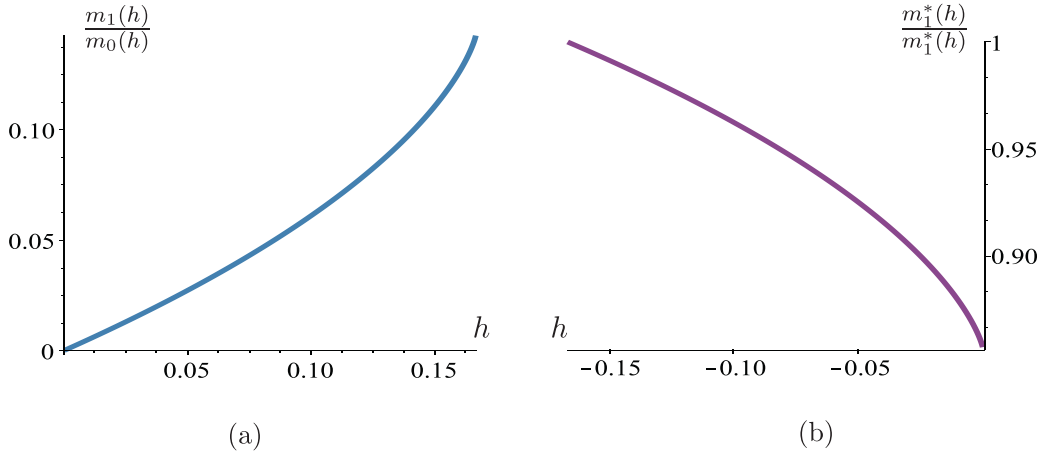


Fig. 2. Simulation of the ratios of elliptic integrals: (a) $\frac{m_1(h)}{m_0(h)}$ for system (25) monotonically increasing in $(0, 1/6)$; and (b) $\frac{m_1^*(h)}{m_0^*(h)}$ for system (27) monotonically decreasing in $(-1/6, 0)$.

Hence, we obtain

$$L'_i(v, Z) \equiv \frac{dL_i(v, Z)}{dv} = \frac{\partial L_i(v, Z)}{\partial v} - \frac{\partial L_i(v, Z)}{\partial Z} \times \frac{\partial v q(v, Z)}{\partial Z q(v, Z)}, \quad i = 0, 1. \tag{39}$$

Then, a direct computation shows that both $L_0(v, Z)$ and the determinant,

$$\begin{vmatrix} L_0(v, Z) & L_1(v, Z) \\ L'_0(v, Z) & L'_1(v, Z) \end{vmatrix},$$

do not vanish on $\{(v, Z) | -\frac{1}{2} < v < 0, 0 < Z < 1\}$. Therefore, $\frac{m_1(h)}{m_0(h)}$ is monotonic for $h \in (0, \frac{1}{6})$ by the Chebyshev criterion [14].

Comparing the proof using the classical B-T bifurcation theory in [13] and that using the dynamical system approach shows that the dynamical system approach is simpler. Moreover, the dynamical system approach can be easily generalized to deal with the case of multiple zeros (multiple limit cycles) in Melnikov functions [12,16].

Moreover, it can be shown that

$$\lim_{h \rightarrow \frac{1}{6}} \frac{m_1(h)}{m_0(h)} = \frac{\int_{\Gamma_0}^* v y d v}{\int_{\Gamma_0}^* y d v} = \frac{1}{7}. \tag{40}$$

Further, by the method and the Maple program in [17] we obtain the asymptotic expansion of $\mathcal{M}(h, \gamma_0, \gamma_1)$ as follows,

$$\mathcal{M}(h, \gamma_0, \gamma_1) = 2\pi \gamma_0 h + O(h^2), \quad \text{for } 0 < h \ll 1,$$

which yields

$$\lim_{h \rightarrow 0} \frac{m_1(h)}{m_0(h)} = 0. \tag{41}$$

Hence, $\frac{m_1(h)}{m_0(h)}$ increases from $(h, \frac{m_1(h)}{m_0(h)}) = (0, 0)$ to $(\frac{1}{6}, \frac{1}{7})$ monotonically, see Figure 2(a). Therefore, $\mathcal{M}(h, \gamma_0, \gamma_1)$ vanishes at any $h = h^* \in (0, \frac{1}{6})$ if $\frac{\gamma_1}{\gamma_0}$ is chosen as $\frac{\gamma_1}{\gamma_0} = -\frac{m_0(h^*)}{m_1(h^*)} \in (-\infty, -7)$. This implies that as the ratio $\frac{\gamma_1}{\gamma_0}$ is varied in the interval $(-\infty, -7)$, a zero of $\mathcal{M}(h, \gamma_0, \gamma_1)$ emerges near $h = 0$ and grows in $(0,1)$.

A similar proof can be given for system (27), and the simulation for $\frac{m_1^*(h)}{m_0^*(h)} = \frac{\int_{\Gamma_h^*}^* v y d v}{\int_{\Gamma_h^*}^* y d v}$ is shown in Figure 2(b).

Summarizing the above results we have the following theorem.

Theorem 1. For the reduced ODE system (25), when $\frac{\alpha_1 - c^2}{c^2 \alpha_5 - \alpha_4} < 0$, a unique limit cycle exists as the ratio $\frac{\gamma_1}{\gamma_0}$ is varied in $(-\infty, -7)$. This unique limit cycle corresponds to a unique periodic wave in the original dispersive-dissipative solid model (7) with external weak dissipation effect, which bifurcates from a stationary state, amplifies and degenerates into a solitary wave.

Further, Hopf bifurcation theory can be applied to easily find the stability of limit cycles bifurcating from the origin of system (35), $(v, y) = (0, 0)$ (i.e., the E_0 of system (33)). Using the method of normal forms (e.g., see [10,15]), we obtain the normal form up to 3rd-order terms for the Hopf bifurcation of system (35) with $M = 1$ and $\Gamma = \gamma_1$, given by

$$\begin{aligned} \frac{dr}{d\xi} &= \frac{1}{2} \epsilon r \left(\gamma_0 + \frac{1}{4} \gamma_1 r^2 \right), \\ \frac{d\theta}{d\xi} &= 1 - \frac{1}{24} (10 + \epsilon^2 \gamma_1^2) r^2, \end{aligned} \tag{42}$$

where r and θ represent the amplitude and phase of motion, respectively. Therefore, the Hopf bifurcation occurs at the critical point $\gamma_0=0$, and is supercritical (or subcritical) if $\gamma_1 < 0$ (respectively $\gamma_1 > 0$), implying that the bifurcating limit cycle is stable (respectively unstable). The transversal condition for the Hopf bifurcation is satisfied, given by

$$H_{\text{trans}} = \frac{1}{2} \epsilon > 0.$$

Moreover, the amplitude and frequency of the limit cycles near the original can be estimated as

$$r = 2\sqrt{-\frac{\gamma_0}{\gamma_1}}, \quad \omega = 1 + \frac{1}{6} \left(\frac{10\gamma_0}{\gamma_1} + 4\gamma_0 \epsilon^2 \right) \approx 1 + \frac{5\gamma_0}{3\gamma_1}, \tag{43}$$

implying that the limit cycle is stable for $\gamma_1 < 0$, which bifurcates from the origin when γ_0 crosses zero from negative to positive.

Similarly, we can obtain the normal form of Hopf bifurcation up to 3rd-order terms for system (27) near the singular point (1,0) as follows:

$$\begin{aligned} \frac{dr}{d\xi} &= \frac{1}{2} \epsilon r \left(\gamma_0 + \gamma_1 + \frac{1}{4} \gamma_1 r^2 \right), \\ \frac{d\theta}{d\xi} &= 1 - \frac{1}{24} (10 + \epsilon^2 \gamma_1^2) r^2. \end{aligned} \tag{44}$$

Remark 2. The unique limit cycle emerges from a Hopf bifurcation when γ_0 is near zero (i.e., when $\frac{\gamma_1}{\gamma_0} \rightarrow -\infty$), and from a Poincaré bifurcation when $|\gamma_0|$ is not small. When choosing the critical value $\frac{\gamma_1}{\gamma_0} = -\frac{m_0(1/6)}{m_1(1/6)} = -7$, the Melnikov integral along the homoclinic loop vanishes, implying the existence of a solitary wave $\Gamma_{0,\epsilon}$, a very little deformation from Γ_0 . A homoclinic loop bifurcation occurs when $\frac{\gamma_1}{\gamma_0}$ crosses the critical value -7 .

It is easy to see from the normal form (42) corresponding to system (25) with $\frac{\alpha_1 - c^2}{c^2\alpha_5 - \alpha_4} < 0$ and the normal form (44) corresponding to system (27) with $\frac{\alpha_1 - c^2}{c^2\alpha_5 - \alpha_4} > 0$ that system (25) can always have Hopf bifurcation since $\gamma_0\gamma_1 < 0$, while system (27) cannot have Hopf bifurcation because

$$(\gamma_0 + \gamma_1)\gamma_1 = \gamma_0^2 \left(1 + \frac{\gamma_1}{\gamma_0} \right) \frac{\gamma_1}{\gamma_0} > 0 \quad \text{for} \quad -\frac{7}{6} < \frac{\gamma_1}{\gamma_0} < -1.$$

Moreover, the Hopf bifurcation for system (25) is supercritical (subcritical) if $\gamma_1 < 0$ ($\gamma_1 > 0$). Since it has been proved that the unique limit cycle exists for the whole interval of the ratio $\frac{\gamma_1}{\gamma_0}$, the conclusion is true in general. Also the stability of the bifurcating limit cycle keeps same for the whole interval. Therefore, we have the following result.

Theorem 3. When $\frac{\alpha_1 - c^2}{c^2\alpha_5 - \alpha_4} < 0$, there exists a unique limit cycle in system (25) as $\frac{\gamma_1}{\gamma_0}$ is varied in $(-\infty, -7)$, and the limit cycle is stable (unstable) if $\gamma_1 < 0$ ($\gamma_1 > 0$). When $\frac{\alpha_1 - c^2}{c^2\alpha_5 - \alpha_4} > 0$, there is no limit cycle bifurcation in system (27).

4. Simulations

In this section, we apply the theoretical results obtained in the previous sections to the PDE system (7) and the corresponding reduced ODE system (25) to study the wave propagations in the model. The data chosen for simulation are taken from [3], given by

$$\alpha_1 = \alpha_3 = \alpha_5 = \alpha_7 = \alpha_8 = \beta_2 = \beta_7 = \beta_8 = 1, \quad \alpha_4 = \beta_6 = 2, \quad \epsilon = 0.1. \tag{45}$$

We first show that these parameter values yield $\frac{\alpha_1 - c^2}{c^2\alpha_5 - \alpha_4} > 0$ for feasible values of c , and thus no limit cycle bifurcation occurs. Then, we change $\alpha_4 = 2$ to $\alpha_4 = 1$ to obtain $\frac{\alpha_1 - c^2}{c^2\alpha_5 - \alpha_4} < 0$ with $\gamma_1 < 0$, yielding stable limit cycles.

Note that in system (7) the coefficients $\alpha_1, \beta_2, \alpha_4, \alpha_5, \beta_6, \beta_7$ and β_8 are positive, while α_3 and α_7 can take positive or negative values. First, consider $\alpha_4 = 2$. We use the above parameter values and the formulas in (22), (24) and (26) to obtain

$$\frac{\alpha - c^2}{c^2\alpha_5 - \alpha_4} = \frac{1 - c^2}{c^2 - 2} \quad \text{and} \quad \frac{\gamma_1}{\gamma_0} = \frac{2(c^2 - 1)(c^2 - 3)}{c^4 - c^2 - 1}.$$

Further, it can be shown that

$$-\infty < \frac{\gamma_1}{\gamma_0} < -7 \implies \frac{1 + \sqrt{5}}{2} < c^2 < \frac{5 + \sqrt{29}}{6} \implies \frac{1 - c^2}{c^2 - 2} > 0$$

which indicates that this case does not belong to system (25) and so by Theorem 3, no limit cycle bifurcation can occur.

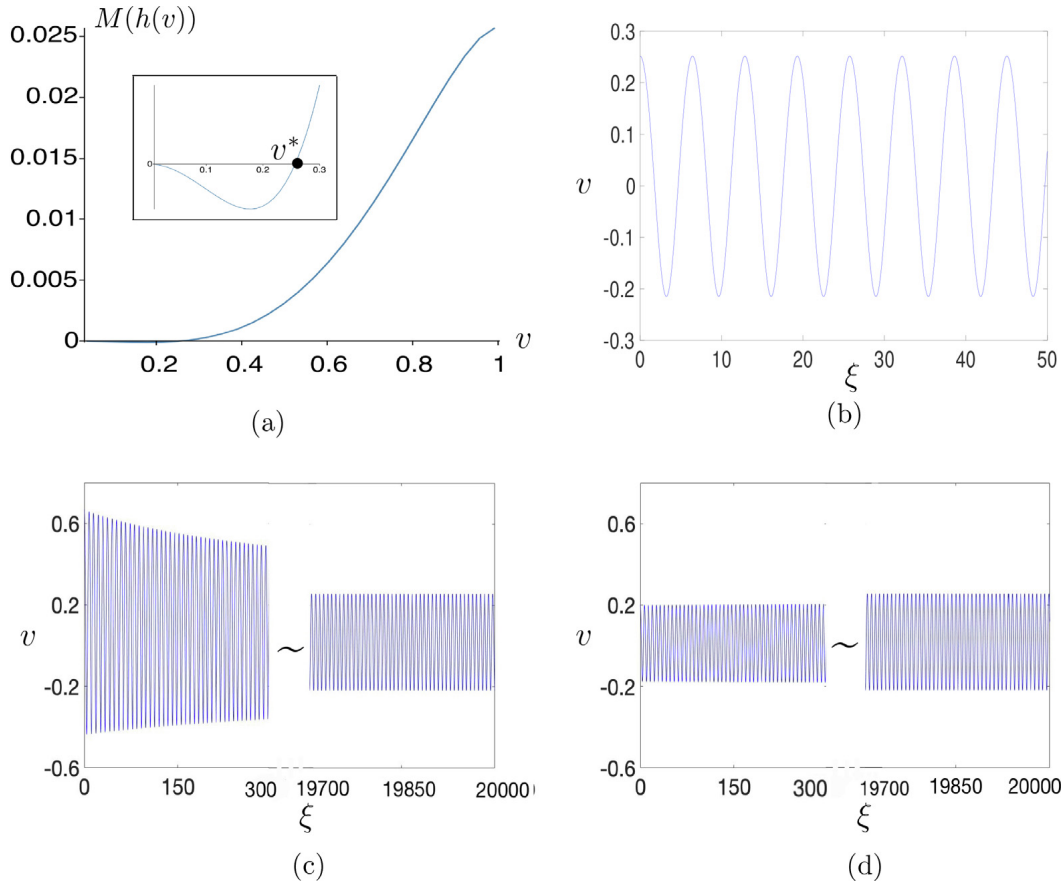


Fig. 3. A simulated periodic orbit of system (25) corresponding to a stationary periodic wave of the model (7) at $c=1/6$: (a) the Melnikov function $\mathcal{M}(h(v))$ has a zero at $v=v^*\approx 0.2516$, as shown in the zoomed figure; (b) a periodic orbit for $v=0.2350$; (c) a wave starting from $v=2/3$ converges to the periodic wave; and (d) a wave starting from $v=1/5$ converges to the periodic wave. Note that the convergence shown in (c) and (d) is very slow.

Next, consider $\alpha_4 = 1$. Similarly, using the parameter values and formulas, we obtain

$$\frac{\alpha_1 - c^2}{c^2\alpha_5 - \alpha_4} = -1 < 0, \quad \text{and} \quad \frac{\gamma_1}{\gamma_0} = \frac{2(c^2 - 1)}{c^2}, \tag{46}$$

implying that this case belongs to system (25) and thus by Theorem 1, a unique limit cycle exists. Using the inequality $-\infty < \frac{\gamma_1}{\gamma_0} < -7$ reveals that

$$0 < c < \frac{\sqrt{2}}{3},$$

which implies that a unique periodic orbit exists for choosing a value of c from the interval $(0, \frac{\sqrt{2}}{3})$. The simulations take $\epsilon = 0.1$ and the results for $c=1/6$ and $c=1/3$ are shown in Figures 3 and 4, respectively, verifying our analytical predictions, though the convergence is slow.

To compare the simulations with the analytical predictions, we first consider the numerical results shown in Figure 3 with $c=1/6$. We use the formulas given in (22), (24) and (26) to obtain $\gamma_0=1/210$ and $\gamma_1=-1/3$, and thus the Hopf bifurcation is supercritical and the bifurcating limit cycle is stable. Moreover, we can use the normal form (42) to estimate the amplitude, r_H , and the frequency, ω_H , of the oscillation as

$$r_H = \frac{2}{\sqrt{70}} \approx 0.2390, \quad \omega_H = 1 - \frac{5}{3 \times 70} = \frac{41}{42} \approx 0.9762.$$

For the oscillation shown in Figure 3(b) obtained using (25) with the initial condition $v = 0.2350$, we have the numerical approximation of the amplitude and frequency, given by

$$v_N \approx \frac{1}{2} [0.2536 - (-0.2161)] = 0.2349, \quad \omega_N = \frac{2\pi}{T} \approx \frac{2\pi}{997.47 - 991.07} \approx 0.9817,$$

which shows a very good agreement with the analytical predictions. Note that v_N is close to the critical value $v^*\approx 0.2516$. For the periodic solution shown in Figures 3(c) and 3(d), obtained using (25) with the initial conditions $v = 2/3$ and $v=1/5$,

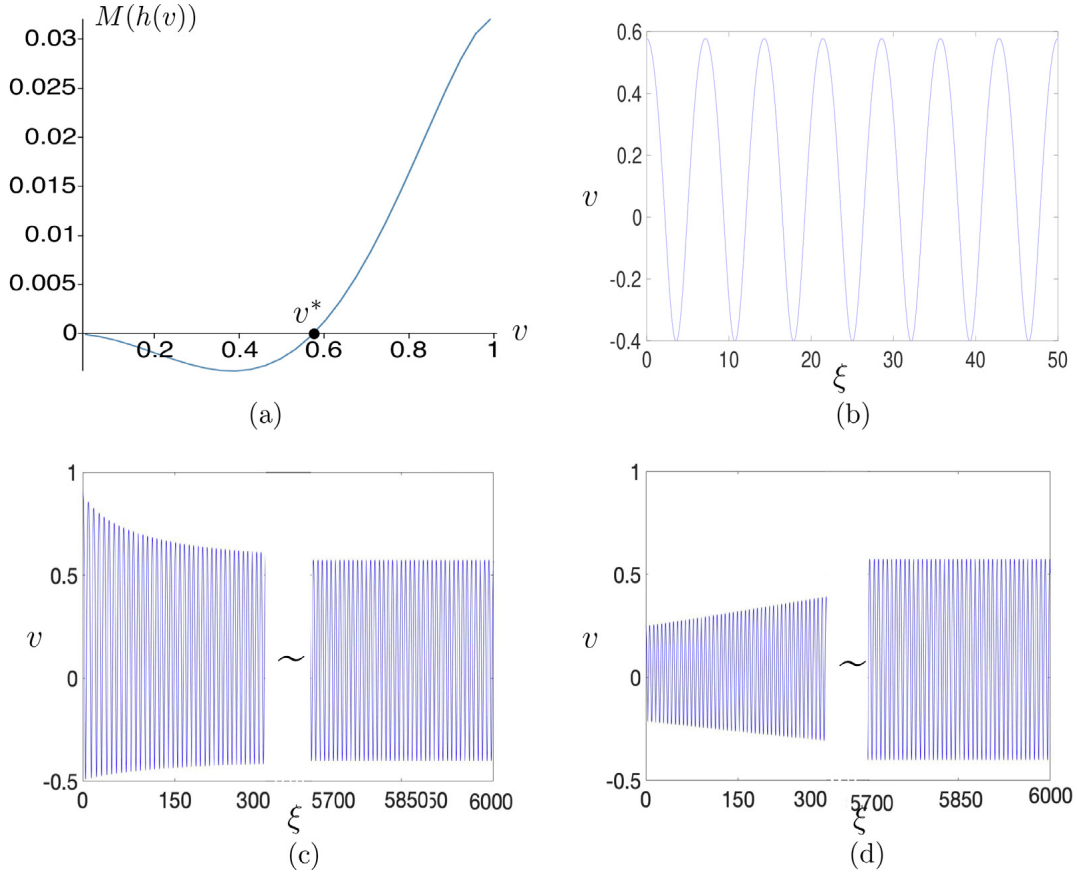


Fig. 4. A simulated periodic orbit of system (25) corresponding to a stationary periodic wave of the model (7) at $c = 1/3$: (a) the Melnikov function $M(h(v))$ having a zero at $v = v^* \approx 0.5779$; (b) a periodic orbit for $v = 0.49$; (c) a wave starting from $v = 100/111$ converges to the periodic wave; and (d) a wave starting from $v = 1/4$ converges to the periodic wave.

we use the numerical results to obtain (taking the average of that given in Figures 3(c) and 3(d))

$$v_N \approx \frac{1}{4} \{ [0.2568 - (-0.2184)] + [0.2568 - (-0.2184)] \} = 0.2376,$$

$$\omega_N \approx \frac{1}{2} \left[\frac{2\pi}{19996.69 - 19990.27} + \frac{2\pi}{19999.31 - 19992.87} \right] = 0.9772,$$

which shows an excellent agreement between these results and the analytical prediction, as well as the simulation given in Figure 3(b).

Similarly, for the results given in Figure 4 with $c = 1/3$, we obtain $\gamma_0 = 1/24$ and $\gamma_1 = -2/3$, which again indicates that the Hopf bifurcation is supercritical and the bifurcating limit cycle is stable. Further, we use the normal form (43) to obtain

$$r_H = \frac{2}{\sqrt{16}} \approx 0.5, \quad \omega_H = 1 - \frac{5}{3 \times 16} = \frac{43}{48} \approx 0.8958,$$

and that for the oscillation shown in Figure 4(b):

$$v_N \approx \frac{1}{2} (0.5779 - (-0.4023)) = 0.4901, \quad \omega_N = \frac{2\pi}{T} \approx \frac{2\pi}{992.31 - 985.21} \approx 0.8850,$$

which again shows an excellent agreement between the prediction and simulation. For the periodic solution shown in Figures 4(c) and 4(d) (again taking the average of that given in these two Figures) we have

$$v_N \approx \frac{1}{4} \{ [0.5747 - (-0.4010)] + [0.5747 - (-0.4010)] \} = 0.4879,$$

$$\omega_N \approx \frac{1}{2} \left[\frac{2\pi}{5985.98 - 5978.82} + \frac{2\pi}{5999.25 - 5992.15} \right] = 0.8812,$$

which also shows a very good agreement between these results and the analytical prediction, as well as the simulation given in Figure 4(b).

The applicability of Hopf bifurcation theory to the results shown in Figures 3 and 4 is easy to be seen from the values of γ_0 , which is $1/210$ for $c = 1/6$ (see Figure 3) and $1/24$ for $c = 1/3$ (see Figure 4), both of them indicates that $0 < \gamma_0 \ll 1$, agreeing with the conclusion that a Hopf bifurcation occurs when γ_0 crosses zero from negative to positive, and it is supercritical for $\gamma_1 < 0$. The stability of bifurcating limit cycles can also be determined from the Melnikov functions shown in Figures 3(a) and 4(a). For Figure 3 (a similar argument for Figure 4), the periodic orbit occurs at $\nu = 0.2350 < \nu^* = 0.2516$, implying that ν is decreasing to pass through the point $\nu = \nu^*$ for which the Melnikov function is decreasing and so the stability of bifurcating limit cycle is stable (see, for example, Chapter 6 in [15]). It should be noted that the stability analysis based on the Melnikov function is not only applicable for Hopf bifurcation (near the center), but also applicable for Poincaré bifurcation (far away from the center), for which Hopf bifurcation theory is not applicable.

5. Conclusion

In this work, a dispersive-dissipative solid model with weakly external dissipation, described by the PDE (7) which does not have analytic solutions, has been analyzed in detail with particular attention on wave solutions. With the GSPT, the model is first reduced to two singularly perturbed ODE systems (25) and (27), and then a detailed analysis is given to show that only system (25) can have limit cycles. Periodic and solitary waves are studied with restriction to a normally hyperbolic manifold. The existence of a unique limit cycle is proved, based on the Alebian integral, first by using the classical B-T bifurcation theory and then by applying a dynamical system approach combined with the Chebyshev criterion. A comparison between these two methods shows that the dynamical system approach is simpler than the traditional B-T bifurcation method, and moreover it can be generalized to deal with Melnikov functions with multiple zeros, i.e., detecting multiple wave solutions. This contribution may promote development of more efficient methodology for studying wave solutions in PDEs.

The theoretical results obtained in this paper are applied to illustrate the application of solving real engineering problems. We consider the model (7) with weak external medium, which was studied in [3] by assuming the existence of a traveling solution. We have presented couple of examples to show that the Melnikov function has a unique zero, yielding a unique traveling wave, verified by simulation. We have found that the traveling solutions are quite sensitive to the parameter values. For example, taking $\alpha_4 = 2$, as used in [3], does not yield wave solutions, while choosing $\alpha_4 = 1$ leads to stable oscillations.

The dynamical system approach combined with the GSPT and Chebchev criterion has been successfully applied to study Melnikov functions which have multiple zeros [16]. Future work is needed to develop a systematic procedure for this approach in order to facilitate the application of this method. Another future work is to investigate the stability of traveling waves, since the stability of limit cycles determined from the reduced ODE system does not necessarily imply the stability of traveling waves of the original PDE model, which may partially depend on the wave's amplitude [8,18].

Declaration of Competing Interest

The authors declare that they have no known competing financial interests or personal relationships that could have appeared to influence the work reported in this paper.

CRedit authorship contribution statement

Xianbo Sun: Investigation, Formal analysis, Writing - original draft. **Yanni Zeng:** Software, Writing - review & editing. **Pei Yu:** Methodology, Software, Writing - review & editing.

Acknowledgment

This research was partially supported by the [Natural Sciences and Engineering Research Council of Canada](#), No. R2686A02 (P. Yu) and the Ontario Graduate Scholarship (X. Sun).

References

- [1] Engelbrecht J. Nonlinear wave motion and evolution equations. *Nonlinear Waves in Solids*. Jeffrey A, Engelbrecht J, editors. New York: Springer; 1994.
- [2] Kerr AD. Elastic and viscoelastic foundation models. *J Appl Mech* 31 1964:491–8.
- [3] Porubov AV, Velarde MG. Dispersive dissipative solitons in nonlinear solids. *Wave Motion* 2000;31:197–207.
- [4] Lurie AI. *Nonlinear theory of elasticity*. Amsterdam: Elsevier; 1990.
- [5] Murnaghan FD. *Finite deformations of an elastic solid*. New York: Wiley; 1951.
- [6] Fenichel N. Geometric singular perturbation theory for ordinary differential equations. *J Differ Equat* 1979;31:53–98.
- [7] Kopell N, Howard LN. Plane wave solutions to reaction-diffusion equations. *Stud Appl Math* 1973;LI(4):291–328.
- [8] Sherratt JA, Smith MJ. Periodic travelling waves in cyclic populations: field studies and reaction diffusion models. *J Royal Soc Interface* 2008;5:483–505.
- [9] Carr J. *Applications of center manifold theory*. New York: Springer-Verlag; 1981.
- [10] Guckenheimer J, Holmes P. *Nonlinear oscillations, dynamical systems, and bifurcations of vector fields* (4th ED.). New York: Springer-Verlag; 1993.
- [11] Kuznetsov YA. *Elements of applied bifurcation theory* (2nd Ed.). New York: Springer-Verlag; 1998.
- [12] Sun X, Huang W, Cai J. Coexistence of the solitary and periodic waves in convecting shallow water fluid. *Nonlinear Anal: Real World Appl* 2020;53:103067.

- [13] Hirschberg P, Knobloch E. An unfolding of the takens-bogdanov singularity. *Q Appl Math* 1991;49:281–7.
- [14] Grau M, Mañosas F, Villadelprat J. A chebyshev criterion for abelian integrals. *Trans Amer Math Soc* 2011;363:109–29.
- [15] Han M, Yu P, Han M, Yu P. Normal forms, melnikov functions, and bifurcations of limit cycles. New York: Springer-Verlag; 2012.
- [16] Sun X, Yu P. Exact bound on the number of zeros of abelian integrals for two hyper-elliptic hamiltonian systems of degree 4. *J Differ Equ* 2019;267(12):7369–84.
- [17] Han M, Yang J, Yu P. Hopf bifurcations for near-hamiltonian systems. *Int J Bifurcat Chaos* 2009;19:4117–30.
- [18] Schnell S, Norbury J. Limit cycles in the presence of convection: a traveling wave analysis. *Phys Rev E* 2007;76:036216.